

## Supplementary Information

# Interlayer-Expanded MoSSe Nanosheets Anchored on Reduced Graphene Oxide for High-Performance Sodium-Ion Batteries

Chen Chen,<sup>a,\*<sup>1</sup></sup> Qilin Hu,<sup>a,1</sup> Yusen Li,<sup>a</sup> Shuya Chang,<sup>a</sup> Lijing Yang,<sup>a</sup> Jinyao Zhou,<sup>a</sup> Siming Jia,<sup>a</sup> Ya Yang<sup>a</sup> and Yongsong Luo<sup>a,b,\*</sup>

a Key Laboratory of Microelectronics and Energy of Henan Province, Henan Joint International Research Laboratory of New Energy Storage Technology, School of Physics and Electronic Engineering, Xinyang Normal University, Xinyang 464000, P. R. China

b School of Physics and Electronic Engineering, Nanyang Normal University, Nanyang 473061, P. R. China

\* The corresponding authors

Email address: chenpaper@outlook.com (C. Chen), ysluo@xynu.edu.cn (Y. Luo).

<sup>1</sup> These authors contributed equally to this work.

**Table of Content:**

**Fig. S1** HRTEM image of the MoS<sub>2</sub>/rGO and MoSe<sub>2</sub>/rGO.

**Fig. S2** SEM images of the MoS<sub>2</sub>, MoSe<sub>2</sub> and MoSSe.

**Fig. S3** CV curves of MoS<sub>2</sub>/rGO electrode and MoSe<sub>2</sub>/rGO electrode at 0.1 mV s<sup>-1</sup>.

**Fig. S4** Cycling performances of the MoSSe electrode at 0.2 A g<sup>-1</sup>.

**Fig. S5** SEM images of the MoSSe/rGO electrodes after 3 cycles, 50 cycles and 100 cycles at 0.2 A g<sup>-1</sup>, respectively.

**Fig. S6** Pseudocapacitance contribution at a scan rate of 1 mV s<sup>-1</sup>.

**Fig. S7** CV curves of MoS<sub>2</sub>/rGO electrode and MoSe<sub>2</sub>/rGO electrode at different scan rates from 0.2 to 1 mV s<sup>-1</sup>. Relationship between log(i) and log(v) of cathodic and anodic peaks. Normalized contribution proportions of capacitance and diffusion of MoS<sub>2</sub>/rGO electrode and MoSe<sub>2</sub>/rGO electrode at different scan rates.

**Fig. S8** GITT profiles of MoSSe/rGO, MoS<sub>2</sub>/rGO, and MoSe<sub>2</sub>/rGO electrodes.

**Fig. S9** Galvanostatic charge/discharge curve at 0.1 A g<sup>-1</sup>. Nyquist plots and R<sub>ct</sub> values of MoSSe/rGO electrode at different potentials.

**Fig. S10** Nyquist plots of MoSSe/rGO, MoS<sub>2</sub>/rGO, and MoSe<sub>2</sub>/rGO electrodes.

**Fig. S11** XRD pattern of Na<sub>3</sub>V<sub>2</sub>(PO<sub>4</sub>)<sub>3</sub>/C.

**Fig. S12** SEM images of Na<sub>3</sub>V<sub>2</sub>(PO<sub>4</sub>)<sub>3</sub>/C.

**Fig. S13** Galvanostatic charge/discharge curves and cycling performances of Na<sub>3</sub>V<sub>2</sub>(PO<sub>4</sub>)<sub>3</sub>/C electrodes at 0.1 A g<sup>-1</sup>.

**Fig. S14** The charge-discharge curves of MoSSe/rGO anode and Na<sub>3</sub>V<sub>2</sub>(PO<sub>4</sub>)<sub>3</sub>/C cathode electrodes at 0.1 A g<sup>-1</sup> in the half-cell.

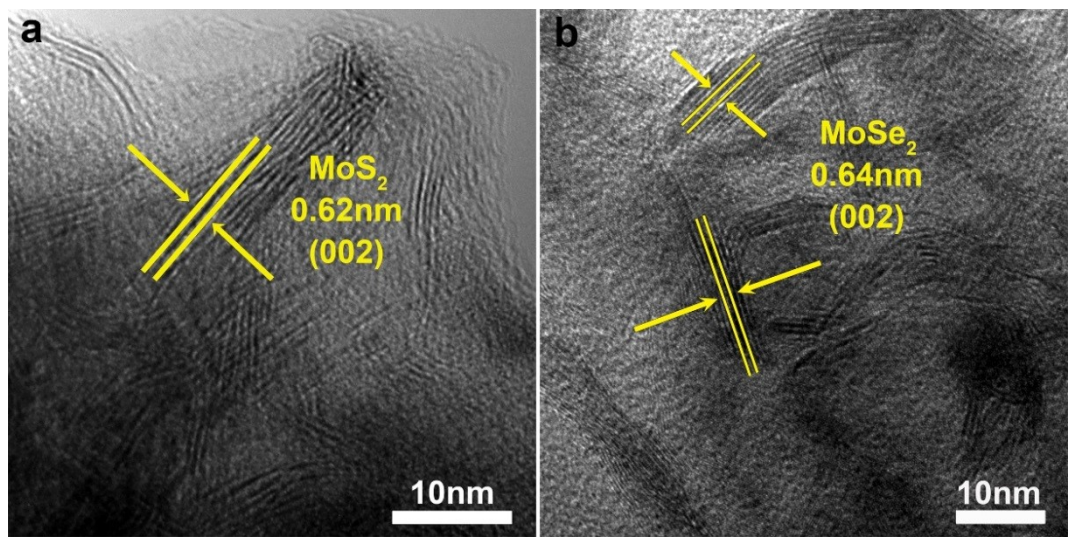


**Fig. S1** HRTEM image of (a) the MoS<sub>2</sub>/rGO and (b) MoSe<sub>2</sub>/rGO.

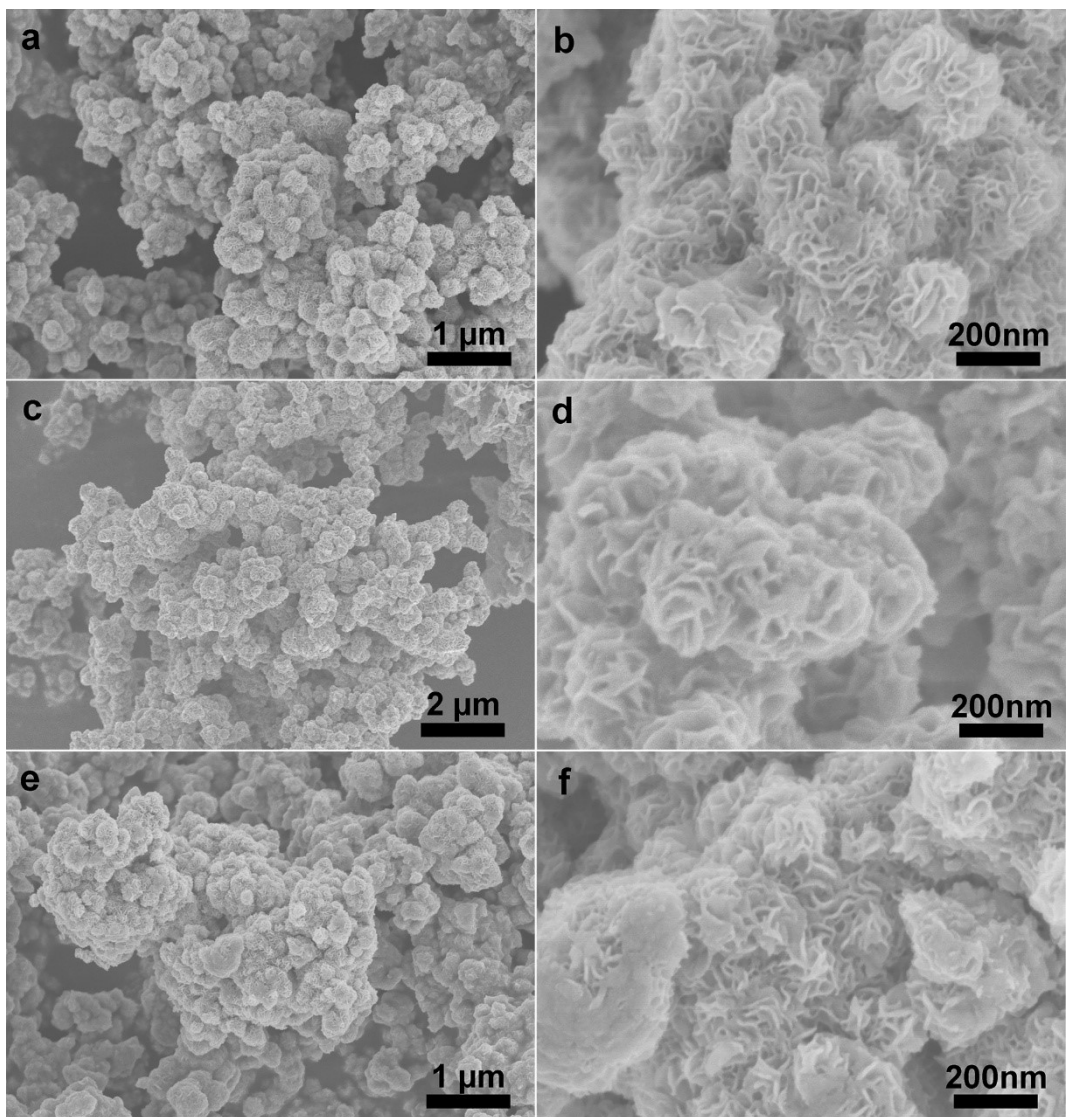


**Fig. S2** SEM images of the (a, b) MoS<sub>2</sub>, (c, d) MoSe<sub>2</sub> and (e, f) MoSSe,

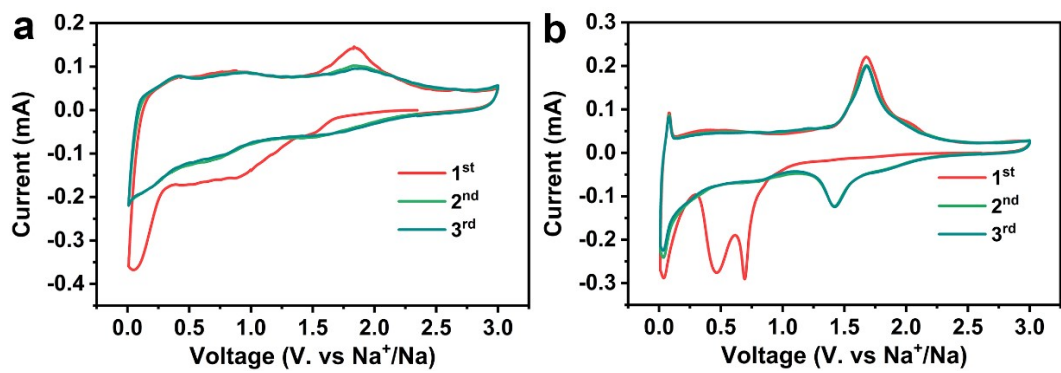


**Fig. S3** CV curves of (a) MoS<sub>2</sub>/rGO electrode and (b) MoSe<sub>2</sub>/rGO electrode at 0.1 mV s<sup>-1</sup>.

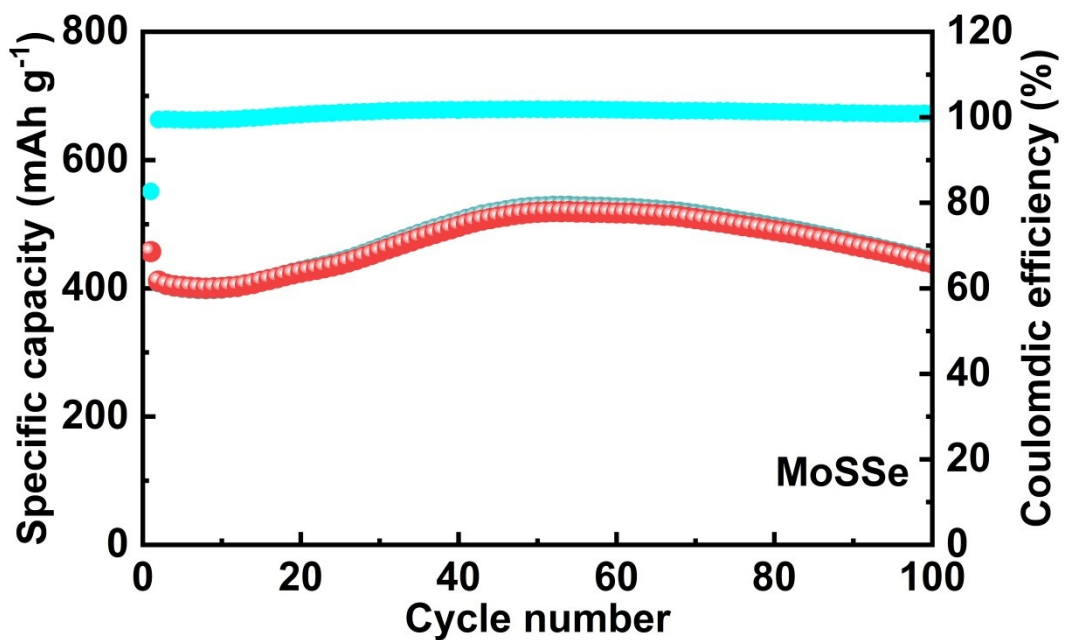


**Fig. S4** Cycling performances of the MoSSe electrode at 0.2 A g<sup>-1</sup>.

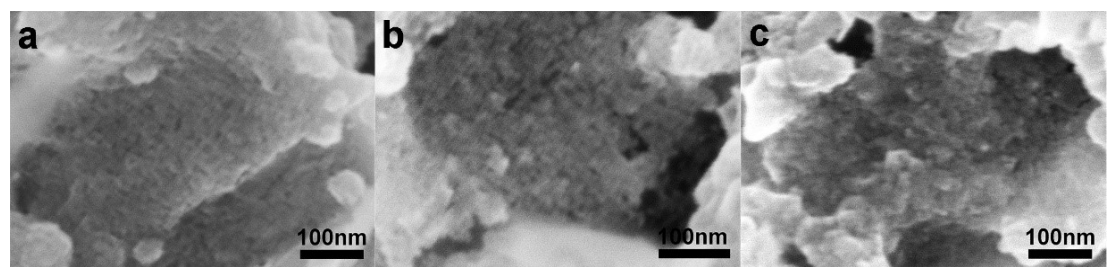


**Fig. S5** SEM images of the MoSSe/rGO electrodes after 3 cycles (a), 50 cycles (b) and 100 cycles at  $0.2 \text{ A g}^{-1}$ , respectively.

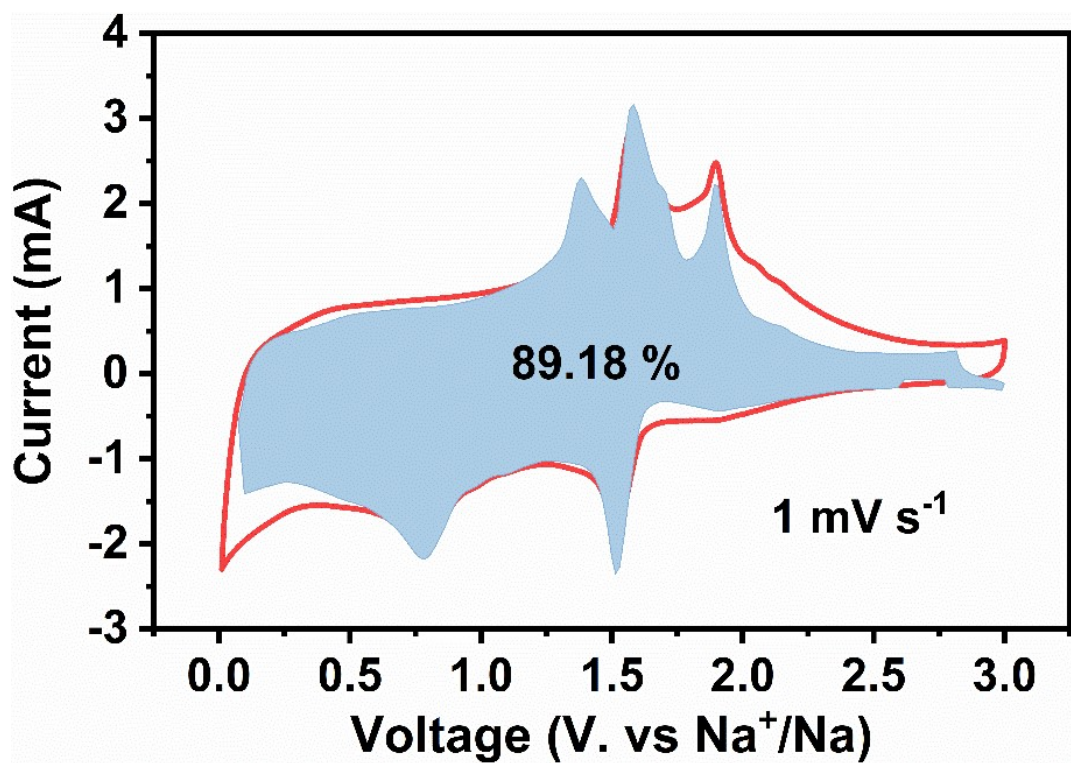


**Fig. S6** Pseudocapacitance contribution at a scan rate of  $1 \text{ mV s}^{-1}$ .

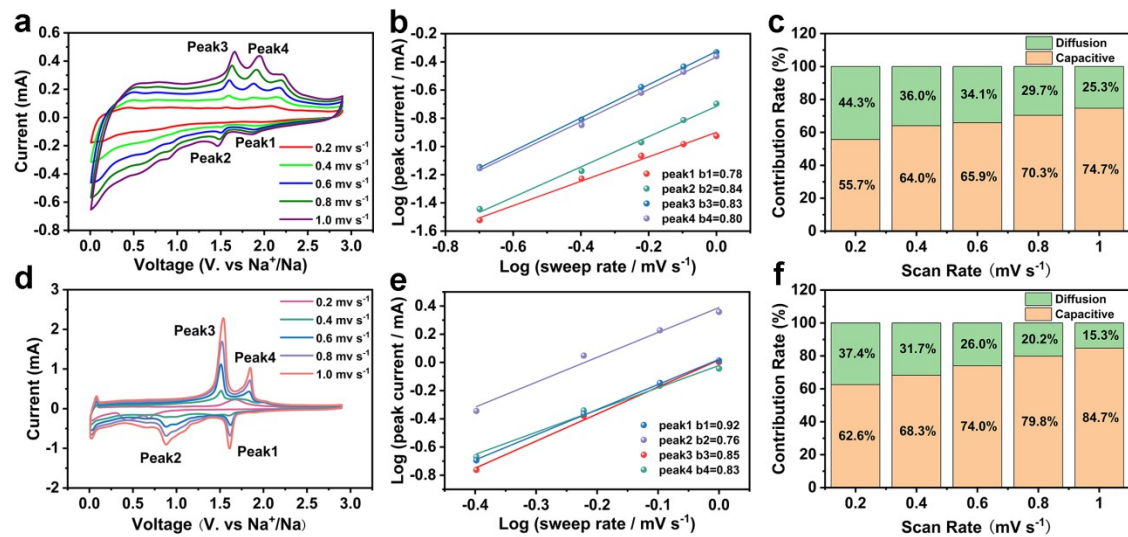


**Fig. S7** CV curves of (a) MoS<sub>2</sub>/rGO electrode and (d) MoSe<sub>2</sub>/rGO electrode at different scan rates from 0.2 to 1 mV s<sup>-1</sup>. Relationship between log(*i*) and log(*v*) of cathodic and anodic peaks of (b) MoS<sub>2</sub>/rGO electrode and (e) MoSe<sub>2</sub>/rGO electrode. Normalized contribution proportions of capacitance and diffusion of (c) MoS<sub>2</sub>/rGO electrode and (f) MoSe<sub>2</sub>/rGO electrode at different scan rates.

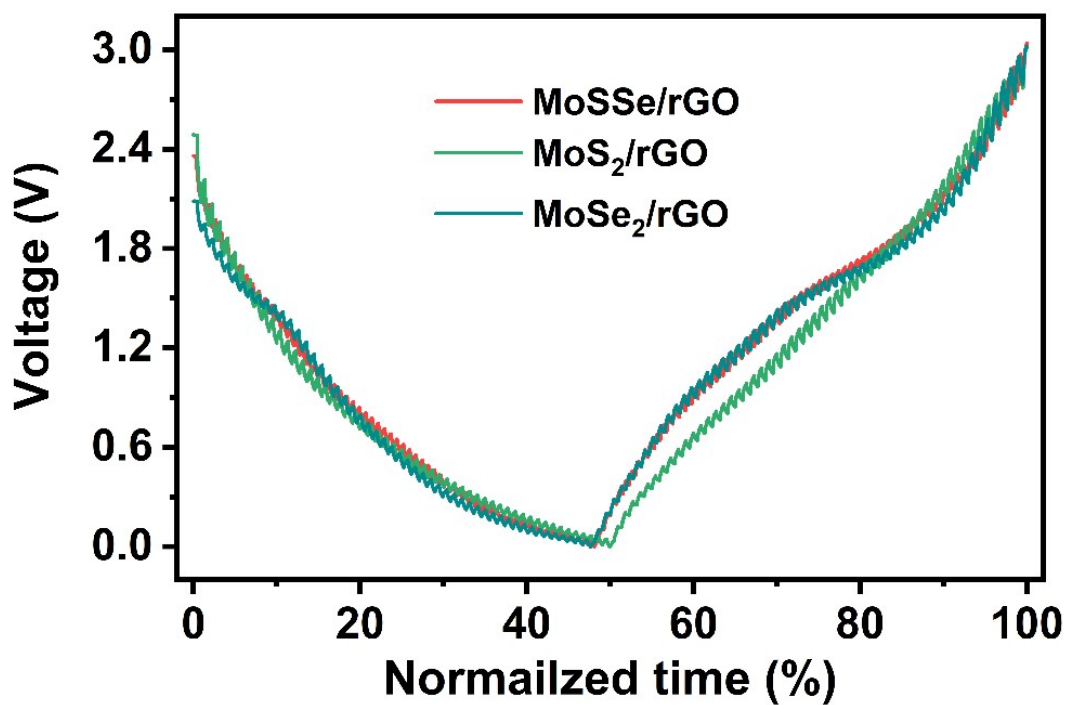


**Fig. S8** GITT profiles of MoSSe/rGO, MoS<sub>2</sub>/rGO, and MoSe<sub>2</sub>/rGO electrodes.

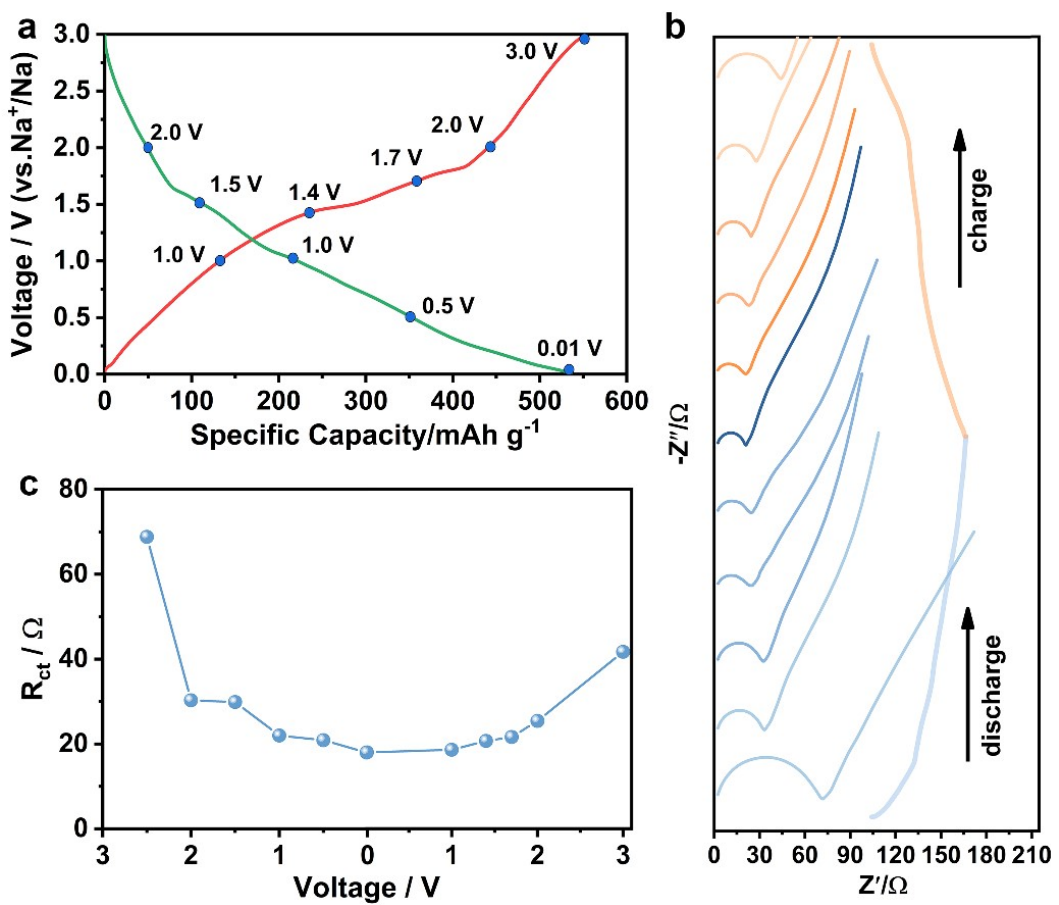


**Fig. S9** (a) Galvanostatic charge/discharge curve at  $0.1 \text{ A g}^{-1}$ . (b) Nyquist plots and (c)  $R_{ct}$  values of MoSSe/rGO electrode at different potentials

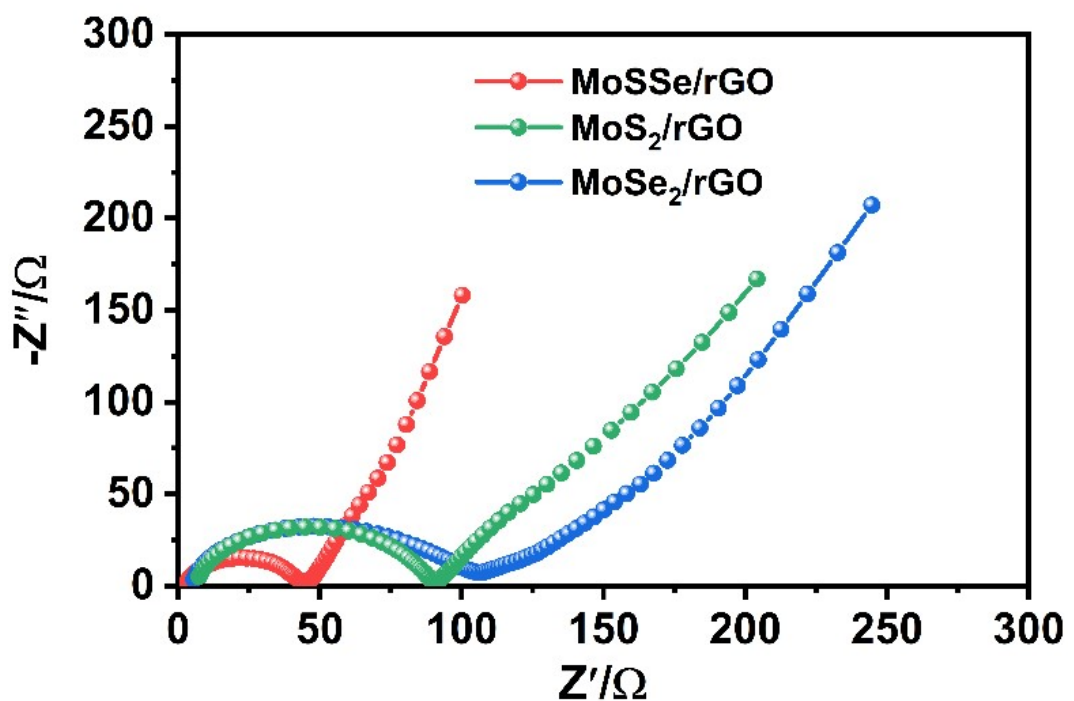


**Fig. S10** Nyquist plots of MoSSe/rGO, MoS<sub>2</sub>/rGO, and MoSe<sub>2</sub>/rGO electrodes.

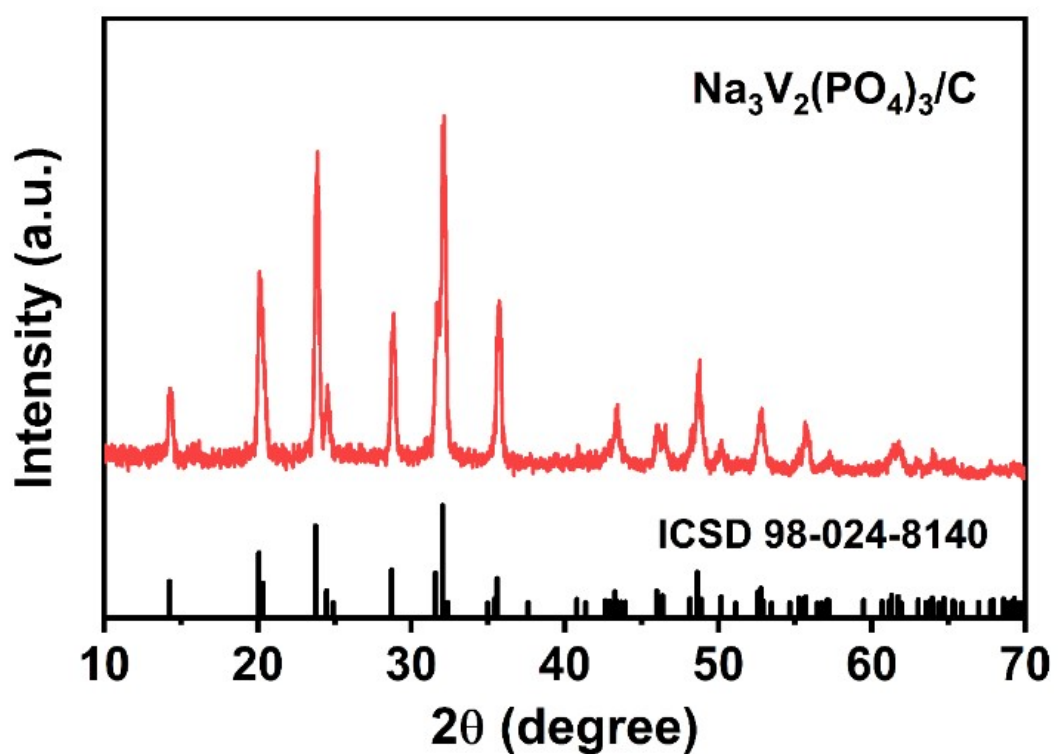


**Fig. S11** XRD pattern of Na<sub>3</sub>V<sub>2</sub>(PO<sub>4</sub>)<sub>3</sub>/C.

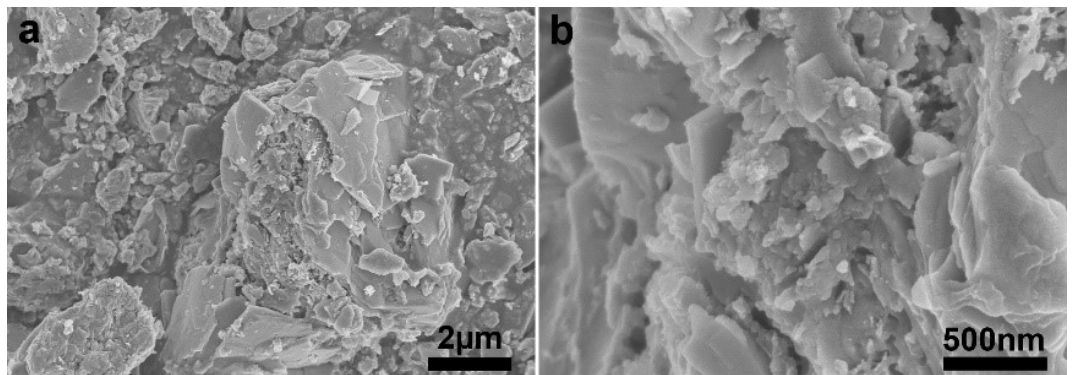


**Fig. S12** (a, b) SEM images of  $\text{Na}_3\text{V}_2(\text{PO}_4)_3/\text{C}$ .

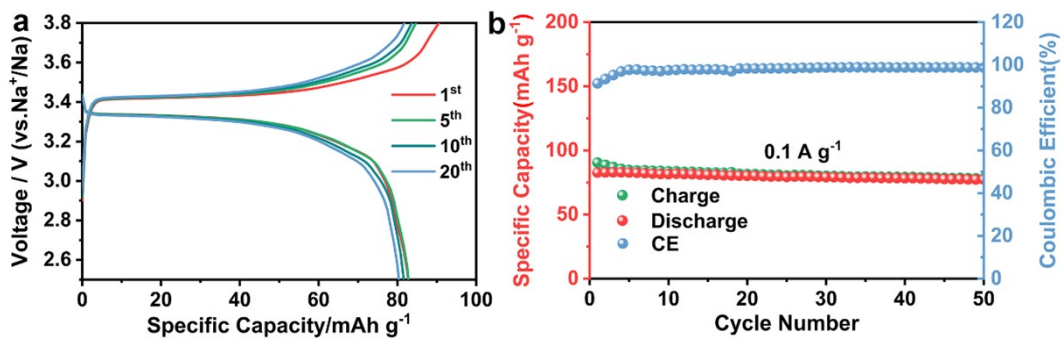


**Fig. S13** (a) Galvanostatic charge/discharge curves and (b) cycling performances of  $\text{Na}_3\text{V}_2(\text{PO}_4)_3/\text{C}$  electrodes at  $0.1 \text{ A g}^{-1}$ .

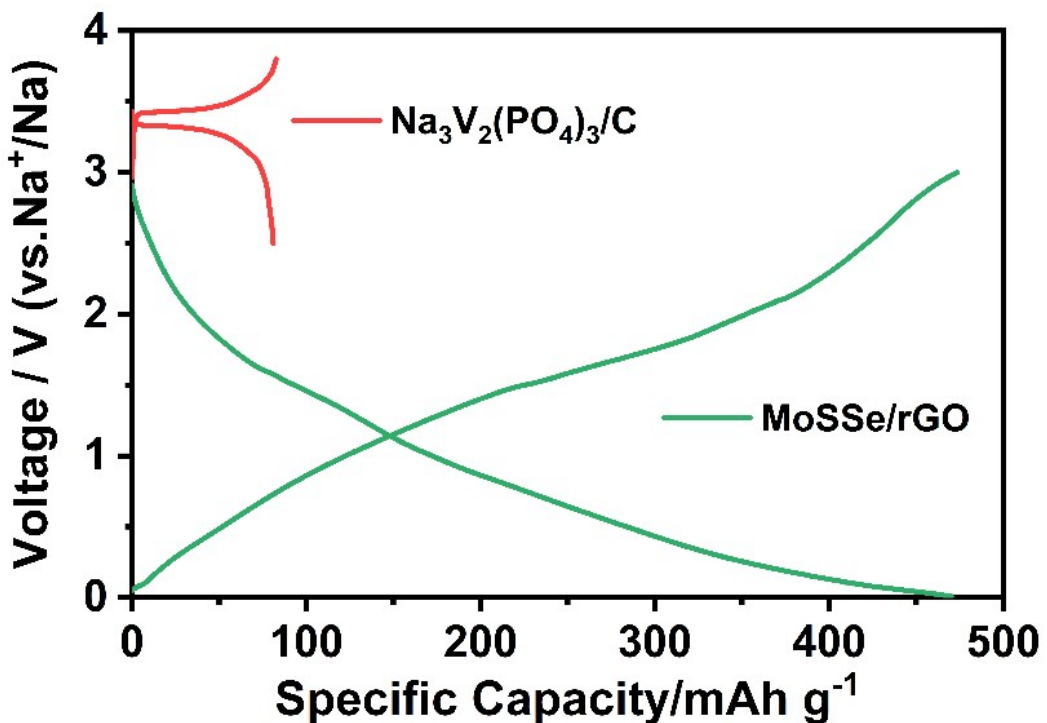


**Fig. S14** The charge-discharge curves of MoSSe/rGO anode and  $\text{Na}_3\text{V}_2(\text{PO}_4)_3/\text{C}$  cathode electrodes at  $0.1 \text{ A g}^{-1}$  in the half-cell.

$$(m_{cathode} \times C_{m(cathode)}) / (m_{anode} \times C_{m(anode)}) = 1.3$$

$$m_{cathode}/m_{anode} = C_{m(anode)} / (1.3 \times C_{m(cathode)}) = 470.2 / (81.0 \times 1.3) = 4.46 \approx 4.5$$

where  $m$  and  $C_m$  are the mass and specific capacity, respectively.